Journal of Colloid and Interface Science **216,** 16–24 (1999)
Article ID jcis.1999.6269, available online at http://www.idealibrary.com on IDEAL®

Transport Properties for Aqueous Sodium Sulfonate Surfactants

2. Intradiffusion Measurements: Influence of the Obstruction Effect on the Monomer and Micelle Mobilities

Onofrio Annunziata, Lucia Costantino, Gerardino D'Errico, Luigi Paduano, and Vincenzo Vitagliano

Dipartimento di Chimica, Università di Napoli, Federico II, via Mezzocannone 4, 80134 Napoli, Italy

E-mail: VITA@chemna.dichi.unina.it

Received July 24, 1998; accepted April 14, 1999

Intradiffusion coefficients of sodium alkylsulfonates [CH_3–$(CH_2)_{n-1}SO_3^-$ Na^+, C_nSNa] (n = 5–9, 11) in mixtures with heavy water were measured by the PGSE-NMR technique at 25°C. A slope change in the experimental trends permits the determination of the critical micelle concentration (CMC). In the micellar composition range, solubilized TMS molecules were used to determine the micelle intradiffusion coefficient, from which the micelle radii were obtained. Both the monomer surfactant and the micelle intradiffusion coefficients show a sharp decrease above the CMC. These results can be interpreted in terms of the obstruction effect due to the micelles. The electrostatic repulsion among charged particles strongly enhances this effect. A simple approach that permits the computation of the Gouy–Chapman layer thickness from the experimental coefficients has been proposed and the results are briefly discussed. © 1999 Academic Press

Key Words: **intradiffusion; micelles; sodium alkylsulfonates.**

INTRODUCTION

The association of amphiphilic molecules into micellar aggregates in aqueous solutions leads to a reduction of the energetically unfavorable contact between water and the apolar parts of the amphiphilic molecules while the polar groups are still solvated by water. Although the hydrophobic interactions among the apolar moieties in the micellar core have been extensively analyzed (1, 2), the understanding of the interactions involving the polar groups is less well developed. The strength of the interactions between the surfactant molecules largely depends on their hydrophilic moieties. In recent years, we have extensively studied micellar systems formed by nonionic ethoxylated tensides (3–6). For dilute solutions of these surfactants, the interactions between the polar heads are weak. On the contrary, for ionic surfactants the electrostatic monomer–monomer, monomer–micelle, and micelle–micelle interactions are important and determine the behavior of the systems (7).

In this paper we present the results of intradiffusion measurements for aqueous solutions of some anionic surfactants of the sodium alkyl sulfonates class [CH_3–$(CH_2)_{n-1}$–SO_3Na, C_nSNa]. These tensides, particularly the shorter ones, have high critical micelle concentration (CMC) values, so that the monomers cannot be neglected and all the above-mentioned interactions must be considered. In these conditions, obtaining unique and reliable values of the micellization parameters is difficult. For this purpose, techniques are required that can distinguish the properties of the micelles from those of monomeric units. From this point of view, transport property measurements seem to be an appropriate experimental approach. The paper presented here is a part of a more extensive work on the transport properties of alkyl sulfonates sodium salts in aqueous solution. In a companion paper mutual diffusion coefficients in the same system are presented and discussed (8). In this work we report and comment on surfactant intradiffusion coefficients. The PGSE-NMR technique provides accurate intradiffusion coefficients for the random thermal motion of surfactants in systems of uniform chemical composition. In the following sections we determine separately the intradiffusion coefficient of both the micellar aggregates and the monomeric units. The diffusion coefficient of micelles extrapolated to infinite dilution is related to their hydrodynamic dimension. Furthermore, we analyze the experimental data and propose a very simple approach to obtaining information on the electrostatic interactions in solution. We think that our data eventually will be useful for testing theoretical treatments for these kinds of systems.

EXPERIMENTAL

Materials. Sigma analytical reagent grade sodium 1-pentanesulfonate [$C_5H_{11}SO_3Na$, C_5SNa], sodium 1-hexanesulfonate [$C_6H_{13}SO_3Na$, C_6SNa], sodium 1-heptanesulfonate [$C_7H_{15}SO_3Na$, C_7SNa], sodium 1-octanesulfonate [$C_8H_{17}SO_3Na$, C_8SNa], sodium 1-nonanesulfonate [$C_9H_{19}SO_3Na$, C_9SNa], and sodium 1-undecanesulfonate [$C_{11}H_{23}SO_3Na$, $C_{11}SNa$] (declared purity ~98%) were dried under vacuum before use and used without

0021-9797/99 $30.00

further purification. The solvent used was D_2O obtained from Sigma (>99.96% isotopic purity). All solutions were prepared by weight. As will be discussed later, solubilized tetramethylsilane (TMS, Sigma, purity 99.9%) was used in the micellar composition range to measure the micelle intradiffusion coefficient.

Intradiffusion measurements. The intradiffusion coefficients were obtained by using the FT-PGSE NMR technique (9, 10). A spectrometer operating in the ^1H mode at 80 MHz and equipped with a pulsed magnetic field gradient unit made by Stelar (Mede, Italy) was used. The Varian spectrometer was modified for better temperature control by using an external refrigeration and water recycling built by RefCon (Naples) according to our design. This equipment provides efficient temperature control of the water cooling the magnet and of the air cooling the sample. A Stelar variable temperature controller (Model VTC87) was used to keep the sample temperature constant within 0.1°C.

The individual spin-echo peak amplitude, A, for a given line is given by

$$A = A_0 \exp\left[-\gamma^2 g^2 \mathcal{D}_a \xi^2 \left(\Delta - \frac{\xi}{3} \right) \right], \qquad [1]$$

where A_0 is a constant for a given set of experimental conditions, γ is the gyromagnetic ratio of the proton, $\mathcal{D}_a$ is the intradiffusion coefficient of the species responsible for the NMR signal, g is the strength of the applied gradient, and Δ and ξ are time parameters in the pulse sequence. The time between the 180° and 90° pulses, Δ, was kept constant. The duration of the two gradient pulses, ξ, was varied over a suitable range to observe the decay of the spin-echo signal A.

The parameters in the above equation were obtained by applying a nonlinear least-squares routine to the decay of A as a function of ξ. In order to evaluate the values of the intradiffusion coefficients, g must be known. Measurements to establish its value were performed on a reference sample with known intradiffusion coefficient; we used heavy water with trace amounts of light water ($\mathcal{D}_{HDO} = 1.872 \times 10^{-9}\ m^2\ s^{-1}$, 11). The sulfonates' intradiffusion coefficients were measured following the signal intensities of the CH_2 groups protons not adjacent to the sulfur atom ($\delta = 1.3$). The experimental errors on the intradiffusion coefficients were generally less than 2%.

In order to correct the intradiffusion coefficients obtained in deuterated solutions back to those in normal water, it is necessary to multiply $\mathcal{D}_a$ by the factor 1.23 (12), which is the ratio of intradiffusion coefficients of normal and deuterated water. Similarly, the molalities in heavy water were multiplied by the $\rho^*_{D_2O}/\rho^*_{H_2O}$ ratio in order to obtain the molalities in light water. The concentrations were computed using the literature density data (8, 13). (No literature data are available for C_8SNa. In this case densities were estimated by interpolating the C_7SNa and C_9SNa data.)

The isotopic substitution of the solvent might result in an alteration of the structural properties of the micellar aggregates. In fact D_2O is thought to be slightly more structured than H_2O (14). Berr (15) showed that these differences are very small and become appreciable only for surfactants with long hydrophobic chains. For this reason we neglected this effect.

RESULTS AND DISCUSSION

The development of explicit theories describing micellar aggregation beyond thermodynamic treatments is a difficult problem because the molecular interactions involved are too complex to be described in terms of statistical mechanics. Thus models are used generally for linking micelle formation to molecular solution structure. These models permit analysis of the experimental data in order to obtain information about the micellization process.

The micellization process of a surfactant can be described as a phase separation (16), so that the concentration of the monomer species becomes constant and equal to the critical micelle concentration (CMC) at higher concentration. For intradiffusion measurements, the CMC determination was discussed in a previous paper (5). Above the CMC, according to this model, the monomer concentration is constant, while the micelle concentration is approximately given by (17)

$$C_M = \frac{C - \mathrm{CMC}}{n}, \qquad [2]$$

where C is the stoichimetric concentration of surfactant, C_M the micelle concentration, and n is the aggregation number.

Alternatively, the micellization process can be described as a chemical equilibrium (18). For anionic surfactants (S^-),

$$nS^- + qM^+ = (S_nM_q)^{-(n-q)} \qquad [3]$$

$$K = \frac{[S_n^- M_q^+]}{[S^-]^n [M^+]^q}, \qquad [4]$$

where M^+ is the counterion and q is the number of counterions bound to each micelle. If n is sufficiently large, the equilibrium model also predicts the onset of micellization in a very narrow range of concentration. However, the monomer concentration does not become constant at higher concentrations.

Both models are simplified models that do not account, for instance, for the polydispersity or for the activity coefficients of the solute species. However, they are good enough to give reasonable insight into the behavior of surfactants solutions through the micellization process (19), although more sophisticated models are described in the literature (20, 21). The choice of the model is mainly related to the discussion of experimental results. We have used both models in the past. For surfactants with short hydrophobic tails, which usually present high and poorly marked CMC values, the properties of

the systems are well described by the equilibrium model. In this work the experimental intradiffusion coefficients are first treated according to the phase separation model. The results permit computation of the equilibrium parameters from the mutual diffusion coefficients (8). These parameters have been used to reanalyze our intradiffusion data to obtain new information about the intermicellar interactions. This is an interesting example in which the combined analysis of intradiffusion and mutual diffusion data largely improve the information that can be obtained from a single technique.

The experimental intradiffusion coefficients are collected in Table 1 and shown in Figs. 1–6. In all cases $\mathcal{D}$ shows a change of slope at the CMC. The measured CMC values are collected in Table 2, where they are compared with some literature values. In the cases of C_9SNa and C_{11}SNa, whose CMCs are very low, we were not able to measure the intradiffusion coefficient in the premicellar composition range.

The intradiffusion coefficients obtained for the C_8SNa aqueous solutions are in very good agreement with those measured by Lindman *et al.* (22).

In the premicellar composition range the intradiffusion coefficients may be fitted as a function of the square root of the ionic strength (23), I, as is usual for electrolyte solutions:

$$\mathcal{D} = \mathcal{D}^{\infty}(1 - \alpha I^{1/2}) \qquad [5]$$

The fitting parameters are reported in Table 2. The intradiffusion coefficients extrapolated to infinite dilution, $\mathcal{D}^{\infty}$, can be compared with those computed by the Nernst relationship,

$$\mathcal{D}^{\infty} = \frac{RT}{\mathcal{F}^2}\,\lambda_-^{\infty}, \qquad [6]$$

where $\mathcal{F}$ is the Faraday constant and λ_-^{∞} is the limiting conductivity of the surfactant anion. Clunie *et al.* (24) obtained λ_-^{∞} for the sodium *n*-alkyl sulfonates from experimental equivalent conductances assuming the limiting conductivity of Na^+, $\lambda_+^{\infty} = 50.10$ ohm^{-1} cm^2, from the literature (25). As one can see in Table 2, the agreement between the experimental and the computed $\mathcal{D}^{\infty}$ is very good.

Actually, these values are different from the limiting coefficients of mutual diffusion. In fact, from the Nernst–Hartley expression, the limiting mutual diffusion coefficient is given by

$$(D^{\infty})_{\text{mutual}} = \frac{2RT}{\mathcal{F}^2}\,\frac{\lambda_+^{\infty}\lambda_-^{\infty}}{(\lambda_+^{\infty} + \lambda_-^{\infty})}. \qquad [7]$$

Given the rapid exchange among free and micellized surfactant molecules, in the micellar composition range the experimental intradiffusion coefficient is a mean value between that of the free monomers, $\mathcal{D}_F$, and that of the micellized molecules, $\mathcal{D}_M$. Thus,

$$\mathcal{D} = p_F\mathcal{D}_F + (1 - p_F)\mathcal{D}_M = \frac{C_F}{C}\,\mathcal{D}_F + \frac{nC_M}{C}\,\mathcal{D}_M, \qquad [8]$$

where p_F is the fraction of amphiphile in the monomeric state and C_F is the free monomer concentration.

For the systems under consideration the $\mathcal{D}$ value decreases sharply above the CMC. The strong $\mathcal{D}$ dependence on concentration is usually attributed to the obstruction effect. In fact the mean square root displacement of a particle decreases if it meets some hindrance in its motion; big particles, like micelles, slow the motion of other micelles and of the free monomer. $\mathcal{D}_F$ and $\mathcal{D}_M$ both depend on the volume fraction of micelles. The presence of charged particles increases this effect because of electrostatic repulsion. As a consequence for ionic tensides:

—the free monomer intradiffusion coefficient, in the micellar composition range, is different from that measured at the CMC, $\mathcal{D}_F^{\text{CMC}}$, where micelles are absent, and shows a dependence on the surfactant concentration;

—the micelle intradiffusion coefficient is not constant.

Micelle intradiffusion coefficients. $\mathcal{D}_M$ can be estimated experimentally by the addition of TMS to the system. In fact, for a compound in a micellar solution which is entirely confined to the micelles and has a negligible solubility in the intermicellar solution, the observed intradiffusion coefficient will be the same as the intradiffusion coefficient of the micelles (26). With this purpose, we added TMS in trace amounts to our solutions. TMS is a strongly hydrophobic molecule and is solubilized in the micellar core. Below the CMC no NMR signal from TMS was observed. This was ascribed to the diffusion of the probe to the air–water interface in the absence of solubilization sites in solution (27). In micellar solutions, electrostatic repulsion should prevent intimate micelle–micelle contacts, barring collisional transfer of solubilized molecules. For these reasons we followed the TMS NMR signal, in order to measure directly the micelle intradiffusion coefficient. The TMS intradiffusion coefficients are collected in Table 1. Inspection of Figs. 1–6 shows that $\mathcal{D}_M \to \mathcal{D}$ as the surfactant concentration increases and the monomeric contribution becomes negligible. As a consequence, it seems realistic to assume that the added solubilizate does not perturb the micelles, i.e., by reducing the CMC or affecting appreciably micelle shape and size.

In a first approximation, the simple pseudo-phase-transition model can be assumed; in this case the micelles start to form at the CMC. This concentration can be considered as the infinite dilution for micelles. Furthermore, the micelle concentration is proportional to the total surfactant concentration minus the CMC (see Eq. [2]). For this reason, the concentration dependence of $\mathcal{D}_M$ can be expanded as a polynomial of $(C - \text{CMC})$,

$$\mathcal{D}_M = \mathcal{D}_M^{\text{CMC}}(1 + A'_M(C - \text{CMC}) + B'_M(C - \text{CMC})^2 + \dots), \qquad [9]$$

TABLE 1
Intradiffusion Coefficients for the Systems D_2O(1)–Surfactant(2) at 298.15 K

C_5SNa			C_6SNa			C_7SNa			C_8SNa			C_9SNa			$C_{11}SNa$		
m (mol kg^{-1})	$\mathcal{D}$ 10^9 (m^2 s^{-1})	$\mathcal{D}_M$ 10^9 (m^2 s^{-1})	m (mol kg^{-1})	$\mathcal{D}$ 10^9 (m^2 s^{-1})	$\mathcal{D}_M$ 10^9 (m^2 s^{-1})	m (mol kg^{-1})	$\mathcal{D}$ 10^9 (m^2 s^{-1})	$\mathcal{D}_M$ 10^9 (m^2 s^{-1})	m (mol kg^{-1})	$\mathcal{D}$ 10^9 (m^2 s^{-1})	$\mathcal{D}_M$ 10^9 (m^2 s^{-1})	m (mol kg^{-1})	$\mathcal{D}$ 10^9 (m^2 s^{-1})	$\mathcal{D}_M$ 10^9 (m^2 s^{-1})	m (mol kg^{-1})	$\mathcal{D}$ 10^9 (m^2 s^{-1})	$\mathcal{D}_M$ 10^9 (m^2 s^{-1})
0.2108	0.551		0.0539	0.573		0.1371	0.517		0.0731	0.519		0.0697	0.508		0.0752	0.157	0.0747
0.3209	0.522		0.0864	0.539		0.1946	0.500		0.0902	0.518		0.0802	0.476		0.0922	0.143	0.0713
0.4919	0.489		0.2803	0.511		0.2348	0.492		0.1010	0.507		0.0904	0.422		0.1060	0.126	0.0700
0.6245	0.464		0.3848	0.471		0.2853	0.482		0.1193	0.510		0.0951	0.397		0.1388	0.102	0.0611
0.8570	0.437		0.5415	0.457		0.3329	0.427		0.1568	0.448		0.1023	0.353		0.1795	0.0797	0.0540
0.9078	0.427		0.6585	0.414		0.3637	0.392		0.1895	0.399		0.1069	0.352		0.2250	0.0651	0.0450
0.9597	0.421		0.7828	0.320		0.4175	0.366		0.2133	0.376		0.1300	0.296				
1.0791	0.408		1.1023	0.244		0.4262	0.333	0.118	0.2561	0.306	0.112	0.1301	0.289				
1.1341	0.389		1.2231	0.184	0.0740	0.4543	0.329		0.2788	0.256	0.100	0.1693	0.246				
1.1984	0.365		1.4841	0.158	0.0557	0.5088	0.285	0.115	0.3302	0.285		0.1734	0.224				
1.2806	0.344		1.6822	0.138		0.5525	0.263		0.3826	0.270		0.2127	0.201	0.0885			
1.3881	0.310		1.8649	0.0950	0.0403	0.5679	0.270	0.106	0.4533	0.165	0.0778	0.2463	0.180	0.0894			
1.3973	0.312		2.1962	0.0846	0.0310	0.6565	0.221		0.4966	0.144	0.0758	0.2970	0.133				
1.5543	0.273		2.4964	0.0593	0.0226	0.7321	0.211		0.5548	0.132	0.0724	0.3420	0.129				
1.7240	0.256					0.7493	0.182	0.0872	0.6528	0.115		0.4379	0.103	0.0600			
1.7523	0.247					0.8376	0.167		0.7951	0.0935	0.0478	0.4580	0.105	0.0627			
1.8447	0.228	0.0797				0.8782	0.165		0.9521	0.0565		0.5510	0.0866	0.0532			
1.9264	0.229					0.9916	0.140	0.0635	1.1230	0.0437	0.0274	0.7038	0.0610	0.0409			
2.2102	0.192	0.0624				1.1962	0.103		1.1620	0.0411	0.0226	1.0092	0.0449	0.0286			
2.3223	0.175	0.0511				1.5450	0.0731	0.0426									
2.6216	0.138	0.0468				2.0220	0.0539	0.0288									
3.0941	0.103					2.5450	0.0462	0.0268									
3.7003	0.0706	0.0168															

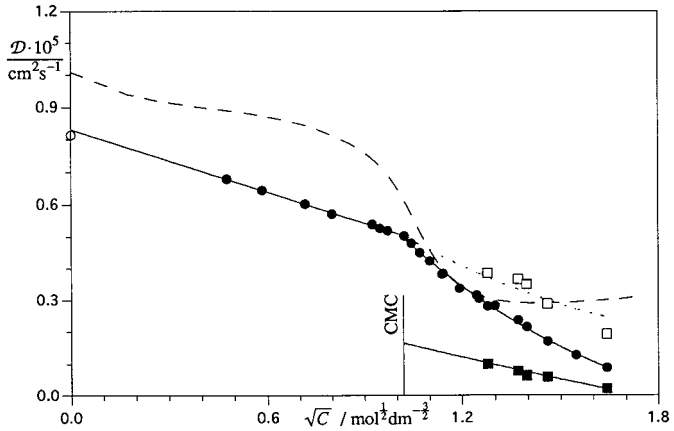

FIG. 1. C_5SNa aqueous solutions: (●) tenside intradiffusion coefficients, (■) TMS intradiffusion coefficients, (○) limiting intradiffusion coefficients computed from conductivity data, (□) free monomer intradiffusion coefficients; the dashed line shows the mutual diffusion coefficient trend.

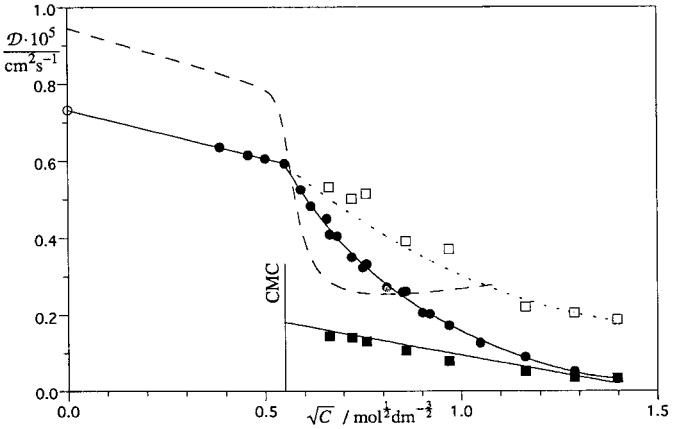

FIG. 3. C_7SNa aqueous solutions: (●) tenside intradiffusion coefficients, (■) TMS intradiffusion coefficients, (○) limiting intradiffusion coefficients computed from conductivity data, (□) free monomer intradiffusion coefficients; the dashed line shows the mutual diffusion coefficient trend.

although the graphs of Figs. 1–6 show that $\mathcal{D}_M$ is almost a linear function of $\sqrt{C}$. Since we are going to discuss the term A'_M later, we collect the fitting parameters of Eq. [8] in Table 3.

It is possible to relate the micelle intradiffusion coefficients, extrapolated at the CMC ($\mathcal{D}_M^{CMC}$), to the hydrodynamic size of the aggregates using the Stokes–Einstein equation to calculate the apparent radius, r (28),

$$r = \frac{k_B T}{6\pi\eta^{CMC}\mathcal{D}_M^{CMC}}, \qquad [10]$$

where η^{CMC} is the viscosity of alkyl sulfonate solutions at the CMC.

In the premicellar solutions of alkyl sulfonate the viscosity follows the relation (29)

$$\eta = \eta^0(1 + BC), \qquad [11]$$

where η^0 is the water viscosity and B is an interpolating coefficient. For a low number of carbon atoms in the hydrocarbon chain, $n_C = 1$–6, the following was found (in mol^{-1} dm^3) (29):

$$B = 0.132 + 0.0843n_C. \qquad [12]$$

For $n_C > 6$, we extrapolated B from Eq. [12]. η^{CMC} was obtained from Eq. [11], with C = CMC; η^{CMC} values are reported in Table 3.

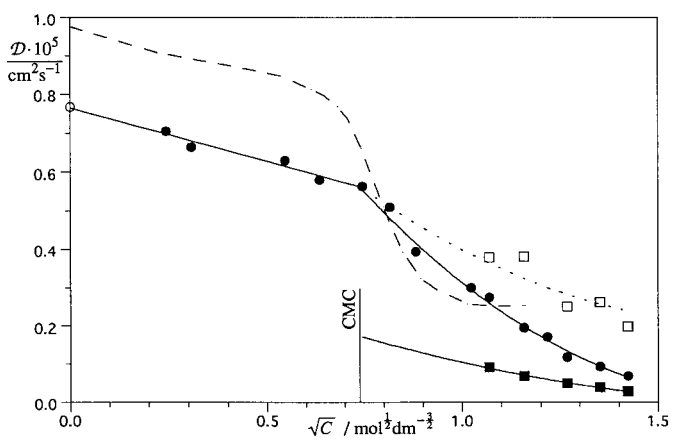

FIG. 2. C_6SNa aqueous solutions: (●) tenside intradiffusion coefficients, (■) TMS intradiffusion coefficients, (○) limiting intradiffusion coefficients computed from conductivity data, (□) free monomer intradiffusion coefficients; the dashed line shows the mutual diffusion coefficient trend.

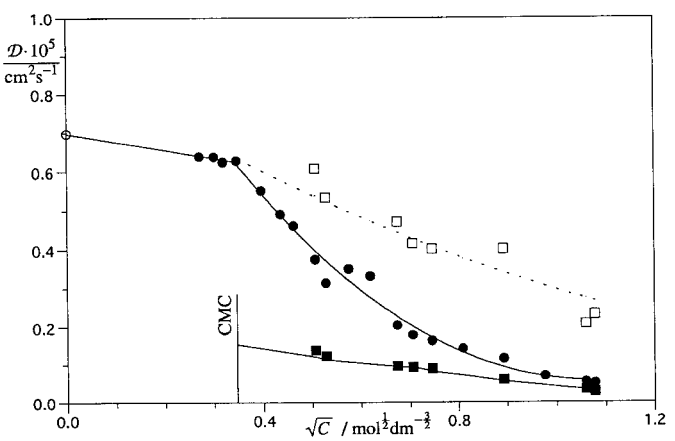

FIG. 4. C_8SNa aqueous solutions: (●) tenside intradiffusion coefficients, (■) TMS intradiffusion coefficients, (○) limiting intradiffusion coefficients computed from conductivity data, (□) free monomer intradiffusion coefficients.

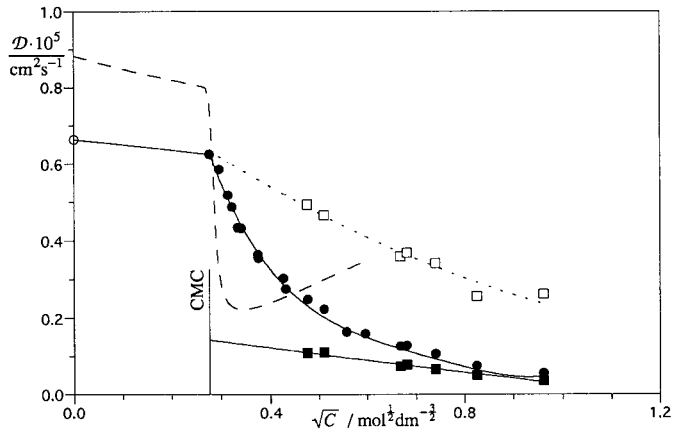

FIG. 5. C_9SNa aqueous solutions: (●) tenside intradiffusion coefficients, (■) TMS intradiffusion coefficients, (○) limiting intradiffusion coefficients computed from conductivity data, (□) free monomer intradiffusion coefficients; the dashed line shows the mutual diffusion coefficient trend.

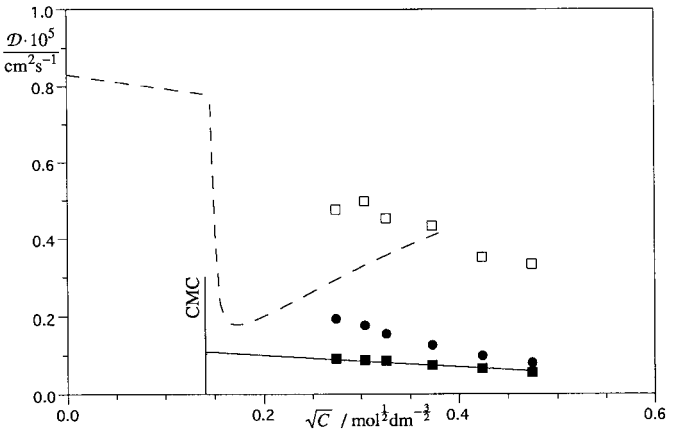

FIG. 6. $C_{11}SNa$ aqueous solutions: (●) tenside intradiffusion coefficients, (■) TMS intradiffusion coefficients, (○) limiting intradiffusion coefficients computed from conductivity data, (□) free monomer intradiffusion coefficients; the dashed line shows the mutual diffusion coefficient trend.

The measured r values are shown in Table 3. They can be compared with those of the alkyl chain length computed according to the Tanford relation,

$$\ell = 0.15 + 0.1265 n_C \qquad [13]$$

where ℓ is approximately the hydrophobic core radius (in nm).

As can be seen, $r > \ell$, with a mean difference of 0.2–0.3 nm, due to the sulfonic heads, the bound counterions, and the hydration water.

$\mathcal{D}_M^{CMC}$ must coincide with the limiting micelle mutual diffusion coefficient (30, 31). The knowledge of $\mathcal{D}_M^{CMC}$ permits the computation of the n, q, and K values for the micellization equilibrium from the mutual diffusion measurements. These parameters permit calculation of the concentration of all species present in solution (8). The results indicate that the free monomer concentration decreases above the CMC. The micelle concentration, C_M, starts to be significant slightly below the CMC and increases linearly with total surfactant concentration. We can reconsider Eq. [9] according to the chemical equilibrium model using the true value of C_M:

$$\mathcal{D}_M = \mathcal{D}_M^{CMC}(1 + A_M C_M + B_M C_M^2 + \dots). \qquad [14]$$

The calculated parameters are reported in Table 4. Clearly, $A_M \approx nA'_M$ and $B_M \approx n^2 B'_M$; however, the results obtained from Eq. [14] must be preferred, considering that the aqueous solutions of our tensides are better described by the equilibrium model.

The concentration dependence of $\mathcal{D}_M$ is generally due to the combination of two effects: intermicellar interactions and change of micelle size. At moderate ionic strength the first effect is prevailing (32, 33). In order to interpret our experimental results, we neglected the second effect.

TABLE 2
Critical Micellar Concentration and Fitting Parameters for the Equations in the Text

	CMC (mol dm^{-3})	CMC (mol dm^{-3})	$\mathcal{D}^\infty\ 10^9$ ($m^2\ s^{-1}$)	$\mathcal{D}^{\infty\,a}\ 10^9$ ($m^2\ s^{-1}$)	α (mol $dm^{-3})^{-1/2}$	n^b	q/n^b	ln K^b
C_5S	1.04	0.99[c]	0.831	0.8132	0.386	9	0.6	−7.00
C_6S	0.540	0.46[c]	0.764	0.7671	0.358	10	0.8	3.40
C_7S	0.302		0.733	0.7322	0.344	12	0.8	18.2
C_8S	0.130	0.14–0.153[c] 0.134[e]	0.697	0.6894	0.295	(17)[d]	(0.8)[d]	(50.1)[d]
C_9S	0.0818	0.06[e]	—	0.6632	0.214	28	0.8	120
$C_{11}S$		0.02[e]	—	0.6027	—	45	0.8	297

[a] Data from Ref. (24).
[b] Data from Ref. (8).
[c] Data from Ref. (44).
[d] Interpolated data.
[e] Data from Ref. (45).

TABLE 3
Fitting Parameters for the Equations in the Text

	$\mathcal{D}_M^{CMC}\ 10^9$ ($m^2\ s^{-1}$)	η^{CMC} (cp)	A'_M ($mol^{-1}\ dm^3$)	B'_M ($mol^{-1}\ dm^3$)	r (nm)	ℓ (nm)
C_5S	0.165	1.40	−0.79	0.157	0.94	0.78
C_6S	0.171	1.20	−0.94	0.257	1.07	0.91
C_7S	0.172	1.08	−1.01	0.320	1.17	1.04
C_8S	0.155	0.984	−1.23	0.436	1.43	1.16
C_9S	0.140	0.955	−1.49	0.707	1.63	1.29
$C_{11}S$	0.106	0.909	−2.46	0.567	2.27	1.44

Although a large body of literature has been developed about the problem of interactions among polyelectrolytes in aqueous solution in the presence and absence of added salts (34–36), only incomplete models have been used so far to describe intermicellar interactions (37, 38). On the other hand, several models have been developed for describing the interaction among uncharged spherical particles. Batchelor (39) has shown that in a dilute suspension of spherical particles it is appropriate to express the intradiffusion coefficient $\mathcal{D}$ as a power series of the particles volume fraction, ϕ. Considering two- and three-body hydrodynamic interactions the following relation holds (40):

$$\mathcal{D} = \mathcal{D}^{\infty}(1 - 1.73\phi + 0.88\phi^2 + \dots). \quad [15]$$

In the following discussion we assume the shape of the micelles to be not very far from the spherical one. Furthermore, we preserve the same dependence on ϕ of Eq. [15] for charged spherical particles. In this case, of course, the particle's volume will appear larger than the real one because of the effect of the electrostatic interactions.

Comparing Eq. [15] and Eq. [14] one can show that

$$A_M = -1.73\,\frac{\phi}{C_M} = -1.73V'_M = -2.31\pi\,\frac{N_A}{10^{24}}\,(r')^3, \quad [16]$$

where V'_M is the excluded volume due to the presence of micelles, r' is the corresponding radius (in nm), and N_A is the Avogadro number. The computed r' values are reported in Table 4. As can be seen $\delta' = r' - r$ is always positive (Table 4). This point will be discussed later.

Monomer intradiffusion coefficients. The free monomer intradiffusion coefficient, $\mathcal{D}_F$, can be computed from Eq. [8]; its trend is shown in Figs. 1–6. $\mathcal{D}_F$ is affected by the ionic strength of the aqueous medium and by the obstruction effect due to the micelles. The former effect can be assumed to be the same as in the premicellar region:

$$\mathcal{D}_F(I) = \mathcal{D}^{\infty}(1 - \alpha I^{1/2}). \quad [17]$$

The ionic strength of the aqueous medium was computed considering the free monomers and counterions concentrations obtained from the equilibrium parameters:

$$I = \frac{1}{2}\,(2C_F + (n - q)C_M). \quad [18]$$

Due to the presence of the charged micelle surface, the ion distribution is not uniform; consequently, the ionic strength computed through Eq. [18] is an approximate value.

Bell (41) proposed a model for taking in account the obstruction effect exerted by spherical micelles on a small particle such as the free monomer,

$$\mathcal{D}_F = \mathcal{D}_F^0(1 + 0.5\phi)^{-1}, \quad [19]$$

TABLE 4
Fitting Parameters for the Equations in the Text

	A_M ($mol^{-1}\ dm^3$)	B_M ($mol^{-1}\ dm^3$)	r' (nm)	δ' (nm)	A_F ($mol^{-1}\ dm^3$)	r'' (nm)	κ^{-1} (nm)	δ'' (nm)
C_5S	−7.03	11.9	1.15	0.21	4.46	1.52	0.274	0.59
C_6S	−9.10	26.8	1.25	0.18	8.58	1.89	0.428	0.85
C_7S	−12.3	46.6	1.39	0.22	12.9	2.16	0.528	1.0
C_8S	−22.1	142	1.69	0.26	21.2	2.55	0.857	1.1
C_9S	−40.4	555	2.06	0.43	51.2	3.49	1.064	1.8
$C_{11}S$	−126	148	3.01	0.74	—	—	1.221	—

where $\mathcal{D}_F^0$ is the monomer intradiffusion coefficient in absence of obstructing particles. This relation holds for uncharged spheres; however, we can preserve this expression for our systems.

As a consequence, $\mathcal{D}_F$ in the micellar region can be interpolated by the following relation:

$$\mathcal{D}_F = \frac{\mathcal{D}_F(I)}{1 + A_F C_M}. \qquad [20]$$

A_F is related to the obstruction effect amplified by the electrostatic interactions. The calculated A_F values are reported in Table 4. Comparing Eq. [20] with Eq. [19], it can be seen that

$$A_F = 0.5\,\frac{\phi}{C_M} = 0.5V''_M = 0.67\pi\,\frac{N_A}{10^{24}}\,(r'')^3, \qquad [21]$$

where V''_M is the apparent molar volume of the micelle, considered as the obstructing object, r'' is the corresponding radius (in nm). In Table 4 the r'' values are reported. Comparing $\delta'' = r'' - r$ with δ', it can be seen that the obstruction exerted by the micelles on the monomers is stronger than that exerted on the other micelles. r' and r'', computed in the composition region near the CMC where the micelle concentration is low, must be considered as indications of the friction encountered, respectively, by the micelle and the monomer to change their position during the diffusion process; i.e., they are hydrodynamic properties. The hydrodynamic volumes can be much larger than the partial molar ones because of the interactions in solution (42). They cannot be assumed as true volumes of actual species in solutions. In fact, using these volumes for computing the space occupied by particles in moderately or highly concentrated solutions, volumes larger than those of the whole solution would be found.

In order to understand the meaning of δ' and δ'', the structure of a micellar system formed by an anionic surfactant must be taken in account. An ionic micelle can be represented as a sperical aggregate whose inner core region consists of methylene tails. The negatively charged headgroups are located on the aggregate surface, in contact with water molecules. The micelle behavior can be described in terms of the polyions theory. The electrostatic potential due to the charges on the micelle surface causes a gradient of the counterion concentration in going from the surface to the bulk solution (34). Oosawa (35) and Manning (36) stated that a fraction of counterions will "condense" on the polyion to lower the charge density of its surface. The adsorbed counterions, along with the surfactant headgroups, form the Stern layer. The residual charge density on the micelle surface produces, on the medium surrounding the micelle, the electric potential

$$\Psi = \Psi^{\circ}\exp(-\kappa x), \qquad [22]$$

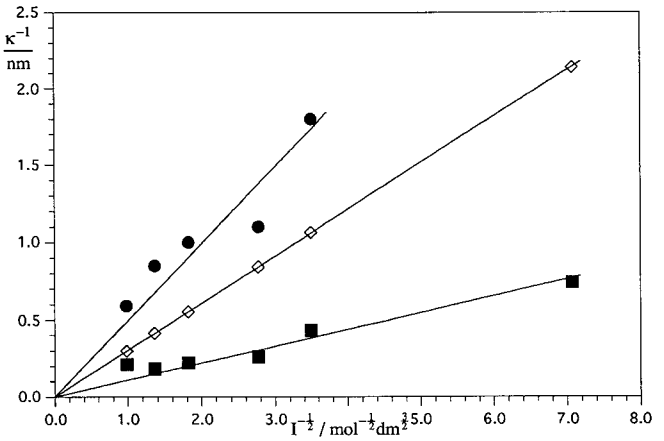

FIG. 7. Gouy–Chapman layer thickness: (●) δ''; (■) δ'; (◇) κ^{-1}.

where x is the distance from the micellar surface, Ψ° is related to the surface charge density, and κ depends on the nature of the intermicellar medium,

$$\kappa^2 = \frac{2000e^2N_A}{\epsilon_0\epsilon_r k_B T}\,I, \qquad [23]$$

where ϵ_0 is the vacuum dielectric constant and ϵ_r is the intermicellar dielectric constant (which we assume to be that of pure water). κ is a linear function of the square root of the ionic strength. Because of the potential given by Eq. [22], near the micelle surface there are excess unbound counterions, while the monomer surfactant anions are rejected. The counterion concentration decreases continuously in going from the micelle surface to the bulk solution.

A simple approximated model is often assumed, in which the excess counterions are confined in a well-defined region surrounding the aggregates, called the Gouy–Chapman layer (43). Its thickness may be identified with κ^{-1}, which has the dimension of length. In Table 2 the computed κ^{-1} values are reported. To estimate κ^{-1}, the ionic strength in Eq. [23] was assumed to be equal to the CMC.

The difference δ'' can be seen as the thickness of the layer surrounding the micelle, where free surfactant anions are hindered from entering because of the electrostatic repulsion due to the micelle charge. In the same manner δ' is the thickness of the layer surrounding the micelle in which another micelle cannot enter because of the repulsion between the two charged surfaces. δ' and δ'' must be proportional to the dimension of the Gouy–Chapman layer.

Inspection of Fig. 7, where κ^{-1}, δ', and δ'' are reported as a function of $I^{-1/2}$ for the surfactants under consideration, shows that δ' and δ'' have the same trend of κ^{-1}. They increase as the ionic strength decreases and are good indices of ionic repulsion. Hence, δ' and δ'' permit a realistic view of the interactions in the micellar systems formed by ionic surfactants.

CONCLUSION

This paper has provided intradiffusion coefficients for an important class of ionic surfactants. The CMCs were determined and in the micellar region both the monomer and the micelle mobilities were determined. They are influenced by the obstruction due to the micelles. This effect is strongly enhanced by the electrostatic interactions in solution.

ACKNOWLEDGMENTS

This research was carried on with financial support of the Italian MURST (Cofin.97 CFSIB) and the Italian CNR.

REFERENCES

1. Tanford, C., "The Hydrophobic Effect," Wiley, New York, 1973.
2. Israelachvili, J. N., Mitchell, D. J., and Ninham, B. N., *J. Chem. Soc. Faraday Trans. II* **72,** 1525 (1976).
3. Ambrosone, L., Costantino, L., D'Errico, G., and Vitagliano, V., *J. Solution Chem.* **25,** 757 (1996).
4. Ambrosone, L., Costantino, L., D'Errico, G., and Vitagliano, V., *J. Solution Chem.* **26,** 737 (1997).
5. Ambrosone, L., Costantino, L., D'Errico, G., and Vitagliano, V., *J. Colloid Interface Sci.* **190,** 286 (1997).
6. Ortona, O., Vitagliano, V., Paduano, L., and Costantino, L., *J. Colloid Interface Sci.* **202,** 000 (1998).
7. Gunnarsson, G., Jönsson, B., and Wennerström, H., *J. Phys. Chem.* **84,** 3114 (1980).
8. Annunziata, O., Costantino, L., D'Errico, G., Paduano, G., and Vitagliano, V., *J. Colloid Interface Sci.* **216,** 8 (1999).
9. Stilbs, P., *Prog. Nucl. Reson. Spectrosc.* **19,** 1 (1987).
10. Callaghan, P. T., "Principles of Nuclear Magnetic Resonance Microscopy," Clarendon Press, Oxford, 1991.
11. Hertz, H. G., *Ber. Bunsen-Ges. Phys. Chem.* **9,** 979 (1967).
12. Goldammer, E. V., and Hertz, H. G., *J. Phys. Chem.* **74,** 3734 (1970).
13. Paduano, L., Sartorio, R., Costantino, L., and Vitagliano, V., *J. Colloid Interface Sci.* **189,** 189 (1997).
14. Nemethy, G., and Scheraga, H. A., *J. Chem. Phys.* **41,** 680 (1964).
15. Berr, S. S., *J. Phys. Chem.* **91,** 4760 (1987).
16. Shinoda, K., and Hutchinson, E., *J. Phys. Chem.* **66,** 577 (1962).
17. Weinheimer, R. M., Fennel Evans, D., and Cussler, E. L., *J. Colloid Interface Sci.* **80,** 357 (1981).
18. Corkill, J. M., Godman, J. F., and Harold, S. P., *Trans. Faraday Soc.* **60,** 202 (1964).
19. Zana, R., "Surfactants Solutions, New Methods of Investigation," Dekker, New York, 1987.
20. Mukerjee, P., *J. Phys. Chem.* **76,** 565 (1972).
21. Desnoyers, J. E., De Lisi, R., Roberts, D., Roux, A., and Perron, G., *J. Phys. Chem.* **87,** 1397 (1983).
22. Lindman, B., Puyal, M., Kamenka, N., Rymdén, R., and Stilbs, P., *J. Phys. Chem.* **88,** 5048 (1984).
23. Mills, R., and Godbole, E. W., *J. Am. Chem. Soc.* **82,** 2395 (1960).
24. Clunie, J. S., Goodman, J. F., and Symons, P. C., *Trans. Faraday Soc.* **63,** 754 (1967).
25. Robinson, R. A., and Stokes, R. H., "Electrolitic Solutions," Butterworth, London, 1955.
26. Jansson, M., and Warr, G. G., *J. Colloid Interface Sci.* **140,** 541 (1990).
27. Jansson, M., and Stilbs, P., *J. Phys. Chem.* **89,** 4868 (1985).
28. Henry, D. C., *Proc. Roy. Soc. A* **133,** 106 (1931).
29. Tamaki, K., Ohara, Y., Kurachi, H., Akiyama, M., and Odaki, H., *Bull. Chem. Soc. Jpn.* **47,** 384 (1974).
30. Sundelöf, L. O., *Ber. Bunsenges. Phys. Chem.* **83,** 329 (1979).
31. Kratohvil, J. P., and Aminabhavi, T. M., *J. Phys. Chem.* **86,** 1254 (1982).
32. Mazer, N. A., Benedek, G. B., and Carey, M. C., *J. Phys. Chem.* **80,** 1075 (1976).
33. Dorshow, R., Briggs, J., Bunton, C. A., and Nicoli, D. F., *J. Phys. Chem.* **86,** 2395 (1982).
34. Fuoss, R. M., Katchalsky, A., and Lifson, S., *Proc. Nat. Acad. Sci.* **37,** 579 (1951).
35. Oosawa, F., *J. Polymer Sci.* **23,** 421 (1957).
36. Manning, G. S., *J. Chem. Phys.* **51,** 924 (1969).
37. Corti, M., and Degiorgio, V., *J. Phys. Chem.* **85,** 711 (1981).
38. Mazo, R. M., *J. Chem. Phys.* **43,** 2873 (1965).
39. Batchelor, G. K., *J. Fluid Mech.* **74,** 1 (1976).
40. Beenakker, C. W. J., and Mazur, P., *Physica* **120A,** 388 (1983).
41. Bell, G. M., *Trans. Faraday Soc.* **60,** 1752 (1964).
42. Ambrosone, L., Della Volpe, C., Guarino, G., Sartorio, R., and Vitagliano, V., *J. Mol. Liq.* **50,** 187 (1991).
43. Hiemenz, P. C., "Principles of Colloid and Surface Chemistry," Dekker, New York, 1986.
44. Mukerjee, P., and Mysels, K. J., Natl. Stand. Ref. Data Ser. (U.S., Natl. Bur. Stand.) No. 36 (1971).
45. Rassing, J., Sams, P. J., and Wyn-Jones, E., *J. Chem. Soc. Faraday Trans. II* **70,** 1247 (1974).